Prediction of combination therapies based on topological modeling of the immune signaling network in Multiple Sclerosis

Authors: Marti Bernardo-Faura[1,2], Melanie Rinas[3], Jakob Wirbel[1,3], Inna Pertsovskaya[4], Vicky Pliaka[5*], Dimitris E Messinis[6], Gemma Vila[4], Theodore Sakellaropoulos[5], Wolfgang Faigle[7], Pernilla Stridh[8], Janina R. Behrens[9], Tomas Olsson[8], Roland Martin[7], Friedemann Paul[9], Leonidas G Alexopoulos[5,6+], Pablo Villoslada[4+], Julio Saez-Rodriguez[1,3+]

[1]European Molecular Biology Laboratory, European Bioinformatics Institute, Cambridge, UK

[2]Centre for Research in Agricultural Genomics (CRAG), Bellaterra, Barcelona, Spain

[3]Joint Research Center for Computational Biomedicine (JRC-COMBINE), RWTH-Aachen University, Faculty of Medicine, Aachen, Germany

[4]Institut d' Investigacions Biomèdiques August Pi Sunyer (IDIBAPS), Barcelona, Spain

[5]National Technical University of Athens, Greece

[6]ProtATonce Ltd, Athens, Greece

[7]University of Zurich, Switzerland

[8]Department of Neurology, Karolinska University Hospital, Sweden and Department of Clinical Neuroscience, Karolinska Institutet, Sweden.

[9]NeuroCure Clinical Research Center and Department of Neurology, Charité University Medicine Berlin, Berlin, Germany

+ **Corresponding authors:**

Julio Saez-Rodriguez, RWTH Aachen University, Faculty of Medicine, MTZ Pauwelstrasse 19,

D-52074 Aachen, Germany. saezrodriguez@gmail.com

Pablo Villoslada, Center Cellex 3A, Casanova 145, Barcelona 08036, Spain. pvilloslada@clinic.ub.es

Leonidas G Alexopoulos, Department of Mechanical Engineering, Building E, Room 301, National Technical University of Athens, Heroon Polytechniou 9, 15780 Zografou, Greece. leo@mail.ntua.gr

Word count: Abstract: 178 words; Text: 5,187 words; References: 41; Figures: 6; Tables: 1; Supplementary figures: 2; Supplementary tables: 8; Supplementary text: 1; Supplementary datasets: 1.

One sentence summary: A new approach to predict combination therapies based on modeling signaling architecture using phosphoproteomics from patients with Multiple Sclerosis characterizes deregulated signaling pathways and reveals new therapeutic targets and drug combinations.

Key Words: signaling networks, pathways, network modeling, logic modeling, kinases, treatment, personalized medicine, combination therapy, Multiple Sclerosis, immunotherapy, phosphoproteomics, xMAP assay

Abstract

Signal transduction deregulation is a hallmark of many complex diseases, including Multiple Sclerosis (MS). Here, we performed ex vivo multiplexed phosphoproteomic assays in PBMCs from 180 MS patients either untreated or treated with fingolimod, natalizumab, interferon-beta, glatiramer acetate or the experimental therapy epigallocatechin gallate (EGCG), and from 60 matched healthy controls. Fitting a bespoke literature-derived network of MS-related pathways using logic modeling yielded a signaling network specific for each patient. Patient models were merged to characterize healthy-, disease- and drug-specific signaling networks. We defined a co-druggability score based on the topology for each drug's network. We used this score to identify kinase interactions whose activity could be reverted to a "healthy-like" status by combination therapy. We predicted several combinations with approved MS drugs. Specifically, TAK1 kinase, involved in TGF-B, toll-like receptor, B-cell receptor and response to inflammation pathways was found to be highly deregulated and co-druggable with four MS drugs. One of these predicted combinations, Fingolimod with a TAK1 inhibitor, was validated in an animal model of MS. Our approach based on patient-specific signaling networks enables prediction of targets for combination therapy for MS and other complex diseases.

Introduction

The signal transduction machinery is frequently involved in perturbations induced by complex diseases. Hence, treatment of complex diseases such as cancer, cardiovascular, immunological or brain diseases is nowadays largely attempted by modulating different molecular cascades involved in the disease to stop disease progression. As such, kinases involved in signaling processes have evolved as primary targets for many diseases (Owens 2007). Further, there has been modest progress with treatments based on single drugs, and combining several drugs targeting different pathways promises more effective modulation of the pathogenic process (Jia et al. 2009; Cully 2015). However, development of combination therapies is hampered by the often incomplete understanding on how their effect propagates through complex signaling networks, with crosstalk between the pathways influenced by each therapy (Klinger et al. 2013; Bozic et al. 2013). As an additional level of complication, disease heterogeneity hinders predicting how a specific combination therapy could be translated into the clinic. Last, the combinatorial nature of such studies in terms of number of targets, drugs, doses, and therapeutic regimen implies a large number of experiments and associated costs, preventing a complete analysis for all alternatives. As a result, the full potential of combination therapies could not be developed. Modeling-based studies may be the key to characterize the effect of drug combinations at the molecular level and allow to predict both efficacy and reduction of off-target effects (Bozic et al. 2013; Korkut et al. 2015; Lee et al. 2012).

Systems biology, and more specifically modeling signaling pathways applied to drug discovery and combination therapy may provide a new path to approach this question (Jia et al. 2009; Villoslada, Steinman, and Baranzini 2009). Mechanistic understanding at the network level offers integrated insights about the cellular responses to environmental changes (Vaga et al.

2014) and drug effects, yielding a significant understanding of the signaling cascades derived from decades of research in this field (Kholodenko, Hancock, and Kolch 2010; Kolch et al. 2015; Davis, Tato, and Furman 2017). Mathematical modeling of signaling networks has been used to unravel signaling mechanisms discover drug targets and disease mediators such as cell surface receptors or intracellular molecules by training those models to experimental measurements of key pathway components in vitro assays using inhibitors and activators (Klinger et al. 2013; Korkut et al. 2015; Palacios et al. 2007).

Multiple Sclerosis (MS) is an autoimmune disease, in which the immune system is chronically activated and damages the central nervous system (CNS) (Ransohoff, Hafler, and Lucchinetti 2015). The involvement of immune system deregulation in MS is shown by altered phenotype and activity of blood lymphocytes and monocytes (Ransohoff, Hafler, and Lucchinetti 2015), as well as by association with genetic polymorphisms of immune genes (International Multiple Sclerosis Genetics Consortium et al. 2011). At present, there are fifteen FDA-approved immunomodulatory drugs, and many others are in late stage clinical development. Most of these control the inflammatory activity in patients with MS to a certain degree, though with known unwanted effects at the signaling level. Furthermore, many unmet medical needs remain in the attempt of achieving control of the disease including more effective therapies, a good safety profile and neuroprotective or regenerative treatments. Drug combinations are considered as a promising strategy to overcome some of these limitations, and in cancer combination therapies are well established (Bayat Mokhtari et al. 2017). However, predicting which patients would benefit the most from a certain combination therapy remains as an unresolved challenge (Kotelnikova et al. 2015; Kieseier and Stüve 2011; Conway and Cohen 2010; Milo and Panitch 2011).

In this study we present a systems medicine approach aimed to (i) characterize the signaling

pathways in primary immune cells obtained from blood of MS patients and controls, and (ii) predict new combination therapies based on the differences in signaling networks between treated MS patients and controls (**Figure 1**). To this end, we assembled a literature- and database-based Prior Knowledge signaling Network (PKN) (Saez-Rodriguez et al. 2009), which includes the pathways involved in immune and MS signaling, as well as their crosstalk and known therapeutic targets. Based on their ability to model large networks with a low number of parameters, logic models have been used to unravel the network topology driving disease and response to therapy (Bernardo-Faura et al. 2014; Eduati et al. 2017; Silverbush et al. 2017; Flobak et al. 2015). Here, we established a Boolean logic model from the signaling network and trained it with measurements of kinase de/phosphorylation as a proxy of signal propagation upon perturbation with ligands and drugs in PBMCs from MS patients and healthy controls. We determined disease- and therapy-specific logic models that characterize the signaling networks for approved treatments (interferon-beta (IFNb), glatiramer acetate (GA), natalizumab (NTZ), fingolimod (FTY) and the experimental drug epigallocatechin gallate (EGCG)). We hypothesized that the signaling interactions that the drugs failed to revert in the *ex vivo* assays to a healthy-like activity level may be candidates to be targeted by a second drug and hence lead to a personalized combination therapy. To identify those reactions, we developed a score of co-druggability of signaling interactions according to quantitative differences in network topology among healthy controls and untreated and treated MS patients (**Figure 1 and Table 1**). Using this network-based approach, we predicted several combination therapies, in particular of TAK1 with 4 MS drugs. We validated a highly-scoring combination therapy in the animal model of MS, experimental autoimmune encephalomyelitis (EAE). The modeling approach shown here can be used for developing combination therapies for other complex diseases as well as for developing personalized therapies.

Results

Multiplexed phosphoproteomic analyses in PBMCs from MS patients and controls

To characterize the signaling networks involved in MS, we created a Prior Knowledge Network (PKN) of biochemical interactions (kinase phosphorylation) reported to be involved in immune signaling associated with MS based on omics- and functional studies, as well as those pathway interactions that were targeted by MS drugs (Kotelnikova et al. 2015). Our network includes pathways such as interferon response, B- and T- cell receptor signaling, cellular survival and apoptosis, lipid signaling, innate immunity and multi-drug response genes (**Figure 2**). To achieve this, we searched in state-of-the-art databases for interactions that were reported in highly specific assays and prioritized experiments with human and PBMC cells (**Supplementary Table S1 and S2**). Further, targets of MS drugs were included into the network via their crosstalk with immune pathways. The PKN featured 167 (**Supplementary Table S2**) proteins and 294 interactions (**Supplementary Table S1**). Subsequently, we developed a multiplex xMAP phosphoprotein panel aiming to maximize the coverage of the MS specific network. The panel, which combined previously and newly developed assays, was then optimized to maximize accuracy, reproducibility as well as network coverage (see **Supplementary Table S3** and **Supplementary Text S1**) (Poussin et al. 2014). After optimization, we selected a set of 17 phosphoproteins with adequate signal to noise ratio that were used for the in vitro assays: AKT1, CREB1, FAK1, GSK3A, HSPB1, IKBA, JUN, MK12, MK03, MP2K1, PTN11, STAT1, STAT3, STAT5, STAT6, TF65, WNK1 (**Supplementary Table S4**). PBMCs were cultured in presence of different sets of stimuli such as lectins, endotoxins, immunostimulants, cytokines and drugs (**Supplementary Table S5**).

We extracted PBMCs from 195 MS patients (mean age: 43.1$\pm$11.3years; disease duration:

8.7±7.7years; median EDSS: 2.0 (0-6.0); subtype: 24 CIS, 129 RRMS, 6 SPMS and 36 PPMS; untreated: 98) and 60 healthy controls (**Supplementary Table S6**). From those 255 patients, 180 were selected and PBMCs were analyzed before stimulation and at 5 and 25 min after stimulation. This yielded a dataset consisting of three measurements for 17 phosphoproteins upon 20 stimuli, to a total of 183600 experimental measurements. For subsequent modeling, the two time points after baseline (5 and 25 min) were collapsed into a single activation signature to define whether a given phosphoprotein was activated or inhibited (see details in methods). Finally, we applied stringent quality control analyses of the dataset consisting of positive and negative controls, reproducibility tests as well as tests for artifacts in the distribution of the samples (see **Supplementary Text S1**), which led to the removal of 2028 data points and 31 patients to generate the final dataset for a total of 169 subjects. After application of identifiability analysis (Saez-Rodriguez et al. 2009), the PKN (shown in **Figure 2**) was reduced to 71 proteins and immune modulators and 168 interactions.

Logic modeling enables characterization of signaling networks in healthy donors and MS patients

Next, we sought to train the generic PKN to these phosphoproteomic measurements in a patient-specific manner to identify each patient's active pathways. To train the same Boolean logic model to the data of each of the 169 subjects, the phosphoproteomic datasets were transformed (**Figure 3A**). To enable comparison of the data to the binary output of the Boolean model, we established a stringent normalization pipeline combining (i) a non-linear transformation to normalize the measurements to continuous values between 0 and 1 while penalizing the outliers (Saez-Rodriguez et al. 2009) with (ii) a statistical filter that removed data-points belonging to proteins that were not found to be significantly phosphorylated or

dephosphorylated (**Supplementary Figure S1**). **Figure 3B** shows the log fold change of each phospho-profile with respect to the control, **Figure 3C** the dataset after the non-linear normalization, and **Figure 3D** displays the proteins found to be significantly dephosphorylated or phosphorylated. Using this normalized dataset, we aimed to identify the active specific signaling network for each subject.

To this end, we fitted a general logic model derived from the PKN (Saez-Rodriguez et al. 2009) to each patient dataset, which resulted in a compendium of 169 models. Model optimization was performed with CellNOpt, a tool that selects the logic model that best matches the data while penalizing model size (Terfve et al. 2012). To increase the robustness of each model, optimization was performed 10 times, and for each patient we selected the best solution as well as all models with a data-to-simulation mismatch within a given relative tolerance reflecting that, due to lack of identifiability and technical noise, different models are feasible (Saez-Rodriguez et al. 2009) (see materials and methods for details). We then built a final model for each patient, defined by the median value of each interaction across all solutions within the relative tolerance (or borders of tolerance) of the best solution (**Figure 4A**).

To confirm that our modeling approach was able to capture the effect on signal transduction of MS drugs, intra- as well as inter-patient model similarities were calculated by the Simple Matching Coefficient (SMC) index. This means, we assessed the number of interactions in two networks that are equal in both networks over the number of all interactions, after stratification of patients by treatment subgroups (**Figure 4B**). Modeling shows that treated MS patients (green boxes) yield more similar signaling activity than untreated MS patients (orange boxes). IFNb-treated patients have a significantly more similar signaling network than untreated RRMS

patients. Treatment with FTY yielded the highest within-subgroup similarity and was statistically more similar in this group's patients than compared to RRMS untreated patients (untreated RRMS mean similarity: 0.737, FTY mean similarity: 0.755, Wilcoxon's test p-value 0.0025). Within-subgroup similarity was also higher for patients treated with IFNb (untreated RRMS mean similarity: 0.737, IFNb mean similarity: 0.750, Wilcoxon's test p-value 7.81 10^{-6}). The large similarity of all solutions found during model optimization for each patient (mean similarity: 0.949) further supported the use of an individual model for each patient. Altogether, these results supported that merging models by subgroups of patients would yield biologically meaningful signaling networks for each group.

We then merged the individual models of healthy donors and separately those of untreated MS patients to characterize MS signaling. We calculated the mean of each interaction for each subgroup and removed the inactive interactions, i.e. those with an activity value below the lower quartile, which we considered neglectable. The differentially activated interactions between healthy donors uncovered signaling pathways deregulated in MS (**Figure 4C)**. Our analysis revealed the activation of several pathways in PBMCs after stimulation both in patients and controls, ranging from cell survival and proliferation, cell adhesion to pro-inflammatory response pathways (e.g. TCR - PAG - CSK - LCK, JAK1 - STAT1, TLR4/IL1R 1- MYD88 - IRAK4 - TRAF6 - TAK1, TRADD - TRAF2 - MAP3K1, SGK - MK03, or RS6 - SGK). Further, pathways such as INSR-PI3K-PIP3-RAF1-AKT1/MP2K1 were found to be activated in MS patients, while BDNF-NTRK1-GRB was found to be activated in healthy donors. These findings indicated that our method was able to identify previously described pathways in the setting of ex vivo analysis of human PBMCs (Kotelnikova et al. 2015), as examined in detail for the individual pathways in the discussion. Untreated MS patients, when compared to healthy controls, showed an increase in the activation of the NFkB pathway (TAK1-IKKB), the

activation of the cell prosurvival PI3K pathway (SLP76-AKT1) or the activation of interferon/cytokines pathways (JAK1-STAT3). Moreover, patients showed a decrease, compared to healthy controls, in the activation of TCR/IL-2 pathway (LCK-STAT1) as well as in the effect of trophic factors signaling on ubiquitination system (EGFR-CBL).

Quantitative differences found in signaling pathways under therapy

We then quantified differences in signaling between patients treated with MS-specific therapies, using the same procedure as for healthy donors vs untreated MS patients. We focused on the strongest signals, i.e. those in the upper quartile of the group mean (**Supplementary Figure S2**), yielding a signaling network of active reactions for each drug-treated subgroup (**Figure 5**).

Interestingly, the activation of TAK1, a key component of the NFKB pathway, was identified in 4 of the 5 networks inferred under treatment, indicating that the NFkB pathway is persistently over-activated by the currently approved MS drugs (**Figure 5A-E**). In the case of IFN-b and GA treated patients, the network revealed the activation by JAK1 of STAT1 and STAT3, whereas EGCG, FTY and NTZ JAK1 regulated the activation of the module via STAT3, STAT6 and STAT1 respectively, and FTY components of the S1PR pathway such as AKT, PLC (**Figure 5B**).

To validate that the therapy-specific pathways found were consistent with the experimental measurements of MS signatures, we quantified the degree to which the original phospho-measurements supported the signaling pathways predicted by modeling for each patient subgroup. The proteins differentially phosphorylated across all stimuli combinations were overrepresented in pathways found by model fitting (IFNb p=1.2E-05; GA p=1.4E-06; FTY

p=0.0004; NTZ p=0.006; Fisher's exact test) except for EGCG, which was limited by the small sample size (**Figure 5F**).

Network topology-based prediction of targeted combination therapy

As our main aim, we sought to use the subgroup networks found to predict novel combination therapies. To this aim, we defined as therapeutic goal to revert the signaling network of patients with MS to a healthy-like activity. We introduced a restriction to our method: the combinations we sought featured one approved MS drug which, in spite of its known efficacy in MS, yielded a signaling activity that differs from the healthy controls as identified by our topological modeling approach. Thereby, we aimed to predict which kinase interactions within the network would revert signaling activity to the healthy-like state when combined with the ongoing therapy. We hypothesized that a co-druggable interaction, i.e. those that a given MS therapy failed to revert to a healthy-like activity level, should be the model interactions with a signaling value more distant between healthy control and MS drug models than between healthy control and MS models (**Figure 1)**. To quantify the co-druggability of each interaction, the quantitative signaling activities predicted for each interaction of untreated MS patients were subtracted from the ones from healthy controls, as well as from the model for each MS drug. This yielded a list of interactions with their corresponding score quantifying co-druggability potential **(Supplementary Table S7 and Supplementary Figure S2**). To identify the co-druggable interactions, we selected those with a negative score as described above, and filtered for additional conditions (see methods and **Supplementary Figure S2**), thereby identifying both the interactions whose signaling activity was different from healthy because of deregulation by the disease as well as because of off-target primary drug effect **(Figure 6A)**. The last step of our approach was to predict the stimulus that would revert to healthy-like the signaling activity of

those interactions identified as co-druggable. Therefore, the co-druggable interactions were mapped onto the signaling network assessed for each subgroup. As an example, **Figure 6B** shows the co-druggable interactions upon FTY treatment mapped onto the FTY network. Mapping the co-druggability for each interaction allowed us to predict combination therapies based on each treatment's signaling network topology. Finally, we employed a graph search approach to identify the in vitro stimulus used in our study that activated interactions found to be co-druggable with each drug by means of a graph search. In other words, we found the experimental readouts that could be measured and reached from an *in vitro* stimulus via an interaction found to be co-druggable *in vivo*. It is important to note that our approach enabled the prediction of combinations of approved MS therapies which yielded a signaling activity distant from healthy controls with drugs that stimulated or inhibited signaling (**Supplementary Table S8**). Interestingly, the activation of IKKB by its ubiquitin-dependent kinase TAK1 was predicted as co-druggable upon treatment with all MS therapies used here in vivo. Among all predictions, we chose to validate the combination of FTY with a TAK1 inhibitor based on (i) the striking signaling homogeneity across FTY models (as quantified in **Figure 4B**), (ii) the finding that TAK1 modulation of HSPB1 via MK12 is largely deregulated (**Supplementary Figure S2**, panel FTY, interaction MK12 - HSPB1) and (iii) the fact that TAK1 is co-druggable in 4 of the 5 drugs.

Validation of combination therapies in the animal model of MS

To validate our approach and obtain an in vivo proof-of-concept of the efficacy of the combination therapies proposed, we sought to assess whether the combination therapies improved the clinical course of the animal model of MS (EAE in the C57BL6 mice immunized with the MOG_{35-55} peptide). Mice were randomized after disease onset (after they reached a

clinical score >1.0), either to placebo (saline), each drug alone (using doses previously demonstrated as efficacious in rodent models) or the combinations of FTY with the TAK1 inhibitor (5Z-7-oxozeaenol). We found that the combination FTY+TAK1-inhibitor ameliorated the clinical course of EAE compared to placebo or to FTY alone (Mann-Withney test; $p<0.05$) (**Figure 6C**). Therefore, our method was able to identify combinations of drugs targeting different pathways that achieved higher efficacy than single therapy.

Discussion

In this study, we applied a modelling approach to characterize signaling activity both at the patient-specific and at the subgroup level. Further, based on the models that encode that activity as well as phosphoproteomic data, we developed a network architecture-based method to predict novel combination therapies for the the treatment of MS. Our algorithm identifies kinase interactions within signaling networks that should be targeted for restoring the network to a healthy-like state, i.e. as a surrogate for therapeutic efficacy (**Figure 1**).

Our approach applied to data from primary immune cells of MS patients allowed us to characterize signaling deregulation in this complex and heterogeneous disease. We identified models of the signaling network for healthy controls, MS patients and for several drugs that are approved for MS. From those models, we used the interactions predicted to be deregulated in MS patients treated with approved drugs to predict combination therapies that can revert the signaling activity to a healthy state at a patient-specific level. In other words, we identified the reactions to be targeted by combination therapy, i.e. the co-druggable interactions. As validation, we tested the combination of one approved drug for MS, namely FTY, with an inhibitor of TAK1, a key component in the predicted signaling networks of 4 out of the 5 in vivo drugs, which was found largely deregulated in FTY. We found that this combination largely

ameliorated the course of the animal model of MS with significantly higher efficacy than the single drug, which provides in vivo proof-of-concept for such combinations. Higher efficacy was obtained using the same doses than individual treatments, hence this approach also provides the opportunity of developing combinations therapies using lower doses to decrease risk of adverse events.

The approach presented here allows insights into signaling deregulation in MS by comparing signaling networks in untreated MS patients with those of healthy controls. The comparison demonstrates higher activation of the NFkB pathway (via TAK1), enhanced pro-survival effects of the trophic factor signaling pathway (AKT1) and modulation of the interferon pathway (JAK1STAT3). In line with the differences found here, aberrant STAT phosphorylation signaling in peripheral blood mononuclear cells from multiple sclerosis patients has also been reported (Canto et al. 2018). The NFkB pathway has been reported to be overactivated in PBMCs from patients with MS (Moreno et al. 2006; Chen et al. 2016) as well as contributing to the genetic susceptibility of the disease (Housley et al. 2015; Hussman et al. 2016). Our analysis supports the pro-inflammatory state of PBMCs in MS at the systems level. The trophic factor pathway involving SLP76 and AKT has also been associated with MS (Kotelnikova et al. 2015) as well as the finding that the MS susceptibility gene CD6 modulates SLP76 (Johnson et al. 2010; Hassan et al. 2006). The involvement may reflect a pro-survival signaling state of T- and B cells in the context of the pro-inflammatory microenvironment. Finally, we observed overactivation of the cytokine/interferon pathway (JAK1), which has previously been reported in MS (Kotelnikova et al. 2015). Moreover, STAT3 has been confirmed as susceptibility gene for the disease (International Multiple Sclerosis Genetics Consortium (IMSGC) et al. 2013), and its activation is impaired in response to IL-10 in MS patients (Martinez-Forero et al. 2008), suggesting a defective response of regulatory Tr1 cells. Regarding the interactions that were

decreased in MS patients compared to controls, PBMCs from patients with MS showed an inhibition of LCK over STAT1 suggesting impairment of the regulation of T/B cell signaling and IL-2 trophic effects (Beyer et al. 2011) or cytotoxicity (Slavin-Chiorini et al. 2004), as well as the regulation of the ubiquitination system modulated by CBL-B (Swaminathan and Tsygankov 2006). LCK is modulated by EVI5, and influences STAT1 in our analysis, both being susceptibility genes for MS (International Multiple Sclerosis Genetics Consortium (IMSGC) et al. 2013). The second inhibited interaction involved the MS susceptibility gene CBL-B (Sanna et al. 2010), which regulates TCR and co-stimulatory signals and regulates immune tolerance through its ubiquitin E3-ligase activity. CBL-B expression is reduced in CD4 cells from MS patients and alters the signaling of the type I interferon pathway (Stürner et al. 2014; Sellebjerg et al. 2012). CBL-B is activated by EGFR, leading to inhibition of several pathways by ubiquitination, including that of EGFR itself (Galisteo et al. 1995; Tarcic et al. 2009). Therefore, our analysis confirmed previous studies identifying deregulation of such pathways in MS (Kotelnikova et al. 2015) and shows the activation of pro-inflammatory pathways and the inhibition of pathways related with immune tolerance. While understanding the biological consequences of such activated and defective interactions would require more detailed studies, these results demonstrate the power of our approach as a tool for interrogating the functional pathways involved in the pathogenesis of this complex disease. Regarding the signaling models of MS drugs, our method is able to identify the activation of pathways downstream of drug targets that were covered in our PKN. Further, it revealed interactions with other disease-associated pathways, which may not directly be involved in the signaling elicited by such drug. Therefore, our modeling approach can be used to provide a wider context of the effects of a given drug on the functions of the target cells. For example, the models identified the activation of JAK1-STAT1 pathway (Pertsovskaya et al. 2013; Schneider, Chevillotte, and Rice 2014) in

IFNb-treated patients, the activation of AKT, PLC (Takuwa et al. 2012; Arish et al. 2017) in patients treated with FTY, or the activation of MAPK, NFkB (via TAK1) (Rose, Alon, and Ginsberg 2007; Abram and Lowell 2009; Luo, Carman, and Springer 2007) in NTZ treated patients.

An important goal of our studies was to develop a modeling approach that can guide the rational development of combination therapies. We hypothesized that the interactions in the subgroup models in response to single drugs that were not reverted to a healthy-like activity state after in vivo treatment should be those with the potential to be co-druggable (**Figure 1)**. Therefore, we developed a co-druggability score that enabled the identification of those interactions and combined that score with a newly developed strategy to predict combination therapies based on network topology. This pragmatic approach has the advantage of allowing prediction of combinations between drugs currently used in patients with MS and compounds that can stimulate signaling where those drugs yield a signaling activity distant from the healthy state. Many strategies have been developed to predict drug combinations (Bulusu et al. 2016). Some have used phosphorylation data upon perturbation using approaches such as applying principal component analysis and partial least square analysis (Lee et al. 2012), data-driven network inference (Bozic et al. 2013; Korkut et al. 2015), or a combination of mechanistic and Bayesian network modeling (Halasz et al. 2016). On the other hand, bottom-up approaches have also been used to predict cancer prognosis from gene-expression profiles that are associated with a deregulated pathways (Crespo et al. 2016). Due to their simplicity, logic networks provide good topological coverage even in the case of large networks and facilitate the dynamic analysis. Thus, they provide a useful framework to study and predict drug combinations (Flobak et al. 2015)(Silverbush et al. 2017; Eduati et al. 2017). In our study we use this logic framework to analyze a large dataset encompassing 183600 data point$_s$ derived from a newly recruited cohort

of 60 healthy donors, and 169 patients, which enabled us to make statements and predictions of direct clinical relevance

Our study has several limitations. First, the analysis of signaling signatures based on phosphoproteomics of mixed immune cells can give rise to high signal variability that is confounded by the presence of multiple cell types. The analysis of signaling abnormalities from specific immune cell subtypes (e.g. CD4+, CD8+, B cells, monocytes) that probably differentially contribute to the disease susceptibility or to the response to therapy may reveal new therapeutic targets. This limitation can be overcome by using mass cytometry in future studies, which allows to collect information on phosphosites from a large number of different cell types and subtypes (Bendall et al. 2012), although at the price of limiting number of subjects (Morris et al. 2014). Nevertheless, by analyzing the cell mixtures contained in PBMCs, we were able to capture the most relevant signals, which would drive immune system activation. Second, our current coverage using validated xMAP assays was restricted to less than 20 kinases, which is a small sample considering the overall number of signaling molecules and pathways that may be activated in immune cells. The availability of robust quantitative phosphoproteomic assays covering hundreds of kinases and signaling molecules in hundred of samples and patients will provide the opportunity of fine tuning the signaling network models for each condition, patient and drug. Third, the Boolean logic approach does not describe processes biochemically and by definition models processes as binary, hence missing subtle aspects of signal transduction (*10*). Our approach is a compromise between data availability, technical feasibility and computational burden that sacrifices details to be able to capture a broad portion of the signaling machinery. Fourth, in this study, we have explored only some of the currently approved drugs for MS patients. The analysis should be extended to those drugs that were recently approved in the future. And fifth, we have averaged individual patients' networks to obtain the subgroup (drug)

network, which leads to losing individual variability, probably related to differential genetic susceptibility or immune system activation. Indeed, we have defined our therapeutic goal in reverting the signaling activity as much as possible the healthy like state. However, this is not the only possible therapeutic approach and disease control may also be obtained by activating or suppressing pathways involved in the control of the pathogenic processes.

In summary, we have developed a topology-based modeling method applied to the understanding of the treatment-specific signaling effects on complex diseases that can be applied to the patient specific level and used for predicting new targets for combination therapy. This approach can be extended to other diseases and optimized to be useful for filtering proposed combination therapies to move to preclinical and clinical testing the most promising candidates.

Materials and Methods

Subjects and clinical cohorts

We recruited 255 subjects including 195 patients with MS and 60 healthy controls, matched for age and sex with the RRMS group, in a multi-centric study in four MS centers (Hospital Clinic Barcelona – IDIBAPS (n=69), Karolinska Institute (n=64), University of Zurich (n=40) and Charité University (n=82)) (**Supplementary Table S5**). Patients fulfilled McDonald 2005 criteria (Polman et al. 2005) and disease subtype was defined using Lublin criteria (Lublin et al. 2014). Patients were allowed to receive any therapy and should be stable in such therapy for the previous 6 months. Patients were recruited by their neurologist after signing informed consent. The study was approved by the IRB of each clinical center.

Samples and processing

A unified standard operating procedure for PBMCs isolation, stimulation and lysis, as well as

sample storing and shipping was developed along with a kit (plates) with reagents and buffers that were produced in a single facility (ProtAtOnce) and shipped to all participating centers (see supplementary text S1 for details). The reagents were prepared from a single batch and plates were prepared from a single batch for each stimulus. Quality controls were carried out to ensure that the reagents remain stable for 3 months.

xMAP assays

XMAP assays were developed by ProtAtOnce (Athens, Greece) and were standardized to minimize error. We optimized assays from a list of 70 candidates (see supplementary text S1) and obtained a final list of 17 phosphoproteins which display a good signal to noise ratio to be measured in the in vitro assays: AKT1, CREB1, FAK1, GSK3A, HSPB1, IKBA, JUN, MK03, MK12, MP2K1, PTN11, STAT1, STAT3, STAT5A, STAT6, TF65, WNK1 (**Supplementary Table S3 and S4**). We used a set of 20 stimuli, which included pro-inflammatory or pro-oxidant stimuli (Anti-CD3, concanavaline A (conA), H2O2, IFNG, IL1A, IL6, LPS, NaCl, PolyIC, TNFA), immunomodulatory stimuli (S1P, vitD3) neuroprotectants or anti-oxidants (BDNF, EGCG, INS and BN201), disease modifying drugs from MS (DMF, FTY, Teriflunomide, IFNB1a (Rebif®)), and a culture media as control (**Supplementary Table S5**). Samples were collected at baseline (time 0) and after 5 and 25 min.

Data normalization

After signal reading, data was normalized (see **Supplementary Text S1**). As described above, data were acquired at 0, 5 and 25 minutes after perturbation. The maximum between 5 and 25 measurements was selected to allow capturing signal transduction including late effects of network motifs such as negative feedback loops. Boolean logic modeling allows simulation for each node in the network as active or inactive. For some perturbations, signals were measured as being activated, inhibited or stay at the same level of phosphorylation as the control. To allow

Boolean modeling of this three-state scenario, differential phosphorylation was calculated and the significant state chosen, thereby discarding the non-significant state and yielding the two most biologically relevant states. This was achieved by testing the log2 Fold Changes (FC) and selecting significant FCs to calculate the signaling activity for each individual interaction in a given patient. Measurements for the same protein that diverged from the significant state were replaced by NA to avoid biasing optimization. Finally, to avoid bias by outliers, a Hill-based non-linear normalization was applied. The normalization algorithm extends from (Saez-Rodriguez et al. 2009) and is shown in **Supplementary Figure S1** and the final dataset with all transformations in **Figure 3**.

Model generation

Healthy controls and MS (untreated) signaling models as well as MS drug-specific models were assembled, using manual curation to prioritize interactions that were found in immune or human cells whenever possible. To allow inclusion of MS drugs, the drug targets were included in pathways as explained above via the references detailed **Supplementary Tables S1 and S2**. The global network featured (168 nodes and 296 interactions). The identifiable components, i.e. those that led to unique solutions using the optimization algorithm, were assessed as described in (Saez-Rodriguez et al. 2009), yielding a so-called preprocessed network of 71 nodes and 168 interactions. Considering that by expanding the logic gates to all possible combinations of 2 or 3 inputs for each AND gate led to an underdetermined modeling, to avoid this, we assessed whether complexes were found between the proteins in the identifiable model. Using an iterative analysis via Bioservices (Cokelaer et al. 2013) and the EBI's complex portal (Meldal et al. 2015) (https://www.ebi.ac.uk/intact/complex), we determined that only the NFkB-IKB complex was present, therefore only this motif was included in the topology. Hence, based on molecular

knowledge the model complexity was reduced to a degree that could be solved by model optimization.

Model Optimization

For each patient, 10 successful optimization runs were performed with a genetic algorithm set to 10 hours, a maximum of 100,000 generations, a population size of 100 individuals, an elitism of 2 individuals propagated through iterations, and a relative tolerance compared to error of the best solution of 0.000005 a.u. After merging all model solutions into a single, robust model for each patient, the resulting patient-specific models were grouped according to treatment and disease subtype. Therefore, the signaling activity calculated for each individual interaction in a given patient was median averaged with the signaling activities of all other patients within the same group for that same interaction.

Network topology-based prediction of combination therapy

To calculate which signaling interaction differed the most when comparing healthy signaling activity and MS patients for each treatment, we calculated the co-druggability score as described in **Figure 1** with *S* indicating the signaling activity status of each interaction:

$$|S_{Healthy} - S_{MS}| - |S_{Healthy} - S_{Treatment}|$$

were *Healthy* refers to assays from healthy controls, *MS* refers to assays done in untreated MS patients and *Treatment* refers to assays done in MS patients treated with approved drugs. Therefore, interactions with a negative co-druggability score indicated a treatment effect that produced signaling activity different to that found in healthy patients and were selected as co-druggable. A co-druggability score of 0 indicated that there was no effect due to drug

treatment.

$$|S_{Healthy} - S_{MS}| - |S_{Healthy} - S_{Treatment}| \leq 0$$

In other words, we used the algorithm described in Figure 1 to define the co-druggability of all interactions within each treatment group after filtering for active signaling. To ensure that interactions with positive scores close to zero were also captured by our method (interactions with a similar signaling activity between drug treatment and MS untreated), we defined an quantile threshold around zero and collapsed almost zero scores into zero. Further, we required co-druggable interactions to be significantly different between healthy and drug signaling. Importantly, applying both filters together allowed our method to identify co-druggable interactions that were deregulated by the disease as well as the unwanted signaling effect by the primary drug.

Table 1 summarizes the score yielded by each combination of healthy-MS-treated signaling activity. This approach enabled to identify the interactions that would require a co-treatment to revert their signaling state to healthy-like (see **Figure 1 for the concept and Figure 6 for the results**).

Experimental Autoimmune Encephalomyelitis

Female C57BL/6 mice from Harlan (8-12 weeks old) were immunized subcutaneously in both hind pads with 300 µg of a myelin oligodendrocyte glycoprotein (MOG_{35-55}, Spikem, Florence, Italy) emulsified with 50 µg of *Mycobacterium tuberculosis* (H37Ra strain; Difco, Detroit, MI,

US) in incomplete Freund´s adjuvant as described previously (Martinez-Pasamar et al. 2013). Mice were injected intraperitoneally with *Pertussis toxin* (500 ng; Sigma, US) at the time of immunization and 2 days later. Animals were weighed and inspected for clinical signs of disease on a daily basis by an observer blind to the treatments. The severity of EAE was assessed on the following scale: 0= normal; 0.5= mild limp tail; 1= limp tail; 2= mild paraparesis of the hind limbs, unsteady gait; 3= moderate paraparesis, voluntary movements still possible; 4= paraplegia or tetraparesis; 5= moribund state; 6= death. Animals (10 mice per arm) were randomized to their treatment once they have reached a clinical score > 1 point. Clinical assessment was performed by a blinded evaluator to the treatment group. Comparison between groups were performed using the Mann-Withney test. * $p< 0.05$.

Statistical analysis of patient subgroup models

to test whether the signaling models found for each patient subgroup were reflected in the experimental phospho-levels, we first calculated for each stimuli pair, if the fold change values (before non-linear normalization) within a single subgroup deviated significantly from 0 by a one-sample Wilcoxon test. Multiple testing correction was performed using the Benjamini-Hochberg strategy. Secondly, we grouped the stimuli pairs into two categories, i.e. either in accordance with the model of signaling or not, by checking if a phospho-readout could be reached by the respective stimulus in the signaling model for the different subgroups (**Figure 5A-E**). Using Fisher's exact test, we then assessed if the stimuli pairs supported by the models were enriched for high significance (using $p<0.05$ as cutoff) compared to the not supported pairs (**Figure 5F**).

Software and data requirements and availability

All presented analyses have been performed with R 3.4.1 and the RWTH computing cluster,

running an LSF job scheduling system, version 9.1.3.0. The CellNOptR package was used in version 1.22.0. All code for the combiMS project can be found on Github (http://github.com/saezlab/combiMS).The experimental dataset is available at CombiMS website (http://www.combims.eu) and eTricks database (http://www.etriks.org).

Acknowledgements

The authors thank Federica Eduati for insightful discussion and valuable advice all along the way. We also would like to thank Thomas Cokelaer for crucial technical help.

Funding: This work was supported by the European Union Seventh Framework Programme: project CombiMS (www.combims.eu), under grant agreement No 305397 as well as Sys4MS project (Horizon2020: Eracosysmed: ID-43). RM and the Section for Neuroimmunology and MS Research, University Zurich (UZH), have been supported by a European Research Council Advanced Grant (ERC 340733-HLA-DR15 in MS), by a Clinical Research Priority Project - disease heterogeneity of MS (CRPP^{MS}; UZH), by the Swiss National Science Foundation and the Swiss MS Society.

Author contributions: Developed the modeling and combination therapy prediction approach: MBF. Conceived and designed the experiments: MBF, IP, VP, DEM, LGA, JSR, PV. Developed new phospho-assays: VP, DEM, TS, LGA. Designed patient cohort and recruited patients: TO, RM, FP, PV. Performed the experiments: VP, DEM, GV, WF, PS, JB. Contributed reagents/materials/analysis tools: MBF, TO, RM, FP, LGA, JSR, PV. Analyzed the data: MBF, JW, TS, JSR. Tested algorithm, performed statistical validation and additional analyses and modified figures accordingly: JW, MR. Wrote the manuscript: MBF. Edited the manuscript: JSR, PV. Supervised the clinical study and experimental validation: PV. Supervised the

modeling, combination therapy prediction and overall project: JSR. All authors revised and approved the final manuscript.

Competing interest: DEM is an employee of ProtATonce; TO has received honoraria for lectures and/or advisory boards as well as unrestricted Multiple Sclerosis research grants from Allmiral, Astrazeneca, Biogen, Genzyme, Merck and Novartis; RM reports grants and personal compensation from Biogen, personal fees from Genzyme Sanofi Aventis, grants and personal fees from Novartis, personal fees from Merck Serono, Roche, Neuway and CellProtect, outside the submitted work; FP has received research grants and personal compensation for activities with Alexion, Bayer, Chugai, Novartis, Merck, Teva, Sanofi, Genzyme, Biogen and MedImmune; LGA is founder and hold stocks at ProtATonce; PV has received consultation fees from Novartis, Roche, Biogen and Genzyme and is founder and hold stocks in Bionure Farma SL, Mintlabs, Health Engineering and Spire Bioventures. He is at present an employee of Genentech, but this work was done before joining Genentech and the company was not involved in this research; All other authors have nothing to disclose.

Data and materials availability: All code and mathematical models are available in Github. Raw data of the xMAP assays is available as supplementary dataset S1 and data is available at eTricks website (http://www.etriks.org).

Figure legends

Figure 1. Topological modeling approach of signaling pathways for prediction of combination therapy. A) Identification of subgroup networks. A model characterizing signaling activity (upstream kinase (circle) that regulates a response e.g. innate immunity, survival (diamond)) in response to a stimulus (oval) was calculated for each subject based on the experimentally acquired dataset. Next, the patient-specific models are merged for all patients

belonging to the same subgroup (left panel blue: healthy controls; middle panel orange: untreated MS; right panel green: treated MS). B) Scoring subgroup interactions to find co-druggable network interactions. The score is calculated to identify interactions that differ from healthy-like signaling activity in spite of drug treatment (see methods). C) Topological prediction of drug combination: A topology-based graph search allows identifying secondary treatments that could target and revert signaling of co-druggable interactions to a healthy-like activity state.

Figure 2. Phosphoproteomic analysis of MS signaling pathways. Reference-based curated MS- and immune-specific Prior Knowledge signaling Network (PKN). Out of the initial 167 signaling components and 294 interaction shown in the figure, 71 and 168 respectively were found to be identifiable by our analysis of the experimental coverage. The shadows indicate the signaling pathways studied, including the crosstalk among them. Blue ovals: experimentally measured phosphoproteins; grey ovals: non-measured phosphoproteins and other molecules involved in signaling; green ovals: stimuli used in the in vitro assays; red lines: inhibitory reactions; black lines: activatory reactions.

Figure 3. Phosphoproteomic measurement- and normalization pipeline. A) xMAP Mean Fluorescence Intensity (MFI) log values of the 17 analyzed phosphoproteins; B) fold change distribution; C) non-linearly normalized values (see methods). Orange measurements A-C: values of the same patient to allow visualization of the changes across data transformation. D) Percentage of patients, for which each phosphoprotein was classified as phosphorylated, dephosphorylated or non-significant after statistical testing.

Figure 4. Logic modeling identifies patient-specific signaling networks and reveals MS-specific signaling pathways. A) Signaling network found by modeling for each patient, visualized as a heatmap. Rows: Single patient network. Columns: Signaling activity estimated

for each interaction by calibrating the PKN shown in Figure 2 after removing the unidentifiable interactions using the phosphoproteomics dataset of each patient. B) Simple Matching Coefficient (SMC) was used to quantify background similarity among all models (All), each model with all solutions for a single patient (Self), and within patient's subgroups (MS drugs: FTY, IFNb, GA, NTZ; experimental drug: EGCG, untreated RRMS (for direct comparison with MS drugs subgroups) and untreated MS (for comparison with healthy controls)). Similarity is higher within each subgroup than compared to background. C) Differentially activated pathways between healthy controls (HC) and untreated MS patients (MS): The models previously calculated for each patient were merged to reveal the common active pathways for controls (blue), untreated MS patients (orange) and both (red). Grey: Inactive interactions from the MS, immune- and treatment-related network (Figure 2).

Figure 5. Signaling networks found for each MS specific therapy. The models previously calculated for each patient were merged to reveal the common active pathways for the experimental drug EGCG and for each MS drug (FTY, IFNb, GA and NTZ) (A-E); F) The differentially phosphorylated proteins were overrepresented (x axis shows the –log adjusted p value) in pathways predicted by modeling as a density score (red line: protein found in model for each corresponding therapy, blue line: absent in that model) and confirmed statistically (see main text).

Figure 6. Combination therapies predicted and *in vivo* validation

A) Co-druggability of all interactions for the MS drugs models. Based on the subgroup models, the co-druggability of all 186 network interactions (X axis) was assessed using the co-druggability score. For each interaction (X axis) the number of drugs (Y axis) is shown, in which it was found to be co-druggable using the co-druggability criteria; B) Total number of

interactions found to be co-druggable for each treatment; C) FTY network co-druggability: the case of FTY network co-druggability is shown as an example (red line: interactions predicted to be co-druggable); D-E) In vivo validation of the combination FTY+EGCG (D) and FTY+TAK1-inhibitor (E) in the EAE model. The graph shows the mean clinical score for each group (n=10). Animals started treatment after disease onset (clinical score >1.0) and were randomized to each treatment and rated in a blinded manner. * $p<0.05$ (Mann-Whitney test).

Table 1. Co-druggability score for all combinations of Healthy-MS-Treated signaling activity. The activity of each signaling interaction was assessed by modeling. The difference between healthy, MS and treated signaling activity (columns 1-3 for a given interaction) was assessed, yielding a score (column 4). The implications for each score are shown in columns 5 and 6**.** Interaction with a negative co-druggability score indicated a treatment effect that produced signaling activity different to that found in healthy patients and were selected as co-druggable. A co-druggability score of 0 indicated that there was no effect due to drug treatment. From those cases, the interactions, in which signaling activity was different between healthy donors and treated patients were also selected as co-druggable, i.e. those where the drug alone failed to revert signaling to a healthy state. Hence, co-druggable interactions were defined as those where treatment with the drug alone yielded signaling activity different to that of the healthy-like state.

List of supplementary materials

1. **Supplementary text S1.** Phosphoproteomics dataset generation.
2. **Supplementary Table S1.** References of the kinase interactions of the Prior Knowledge Network (PKN)
3. **Supplementary Table S2.** List of the phosphoproteins selected from the literature search, the stimuli applied and the MS drugs used for building the Prior Knowledge Network (PKN)
4. **Supplementary Table S3.** Selection of phosphoproteins based in their involvement in pathways associated with MS or MS drugs and assays performance. Phosphoproteins for the xMAP assays were selected based in a good signal to noise ratio to maximize network coverage and model identifiability
5. **Supplementary Table S4.** List of phosphoproteins used for in vitro multiplex assays with PBMCs
6. **Supplementary Table S5.** Stimuli used for the in vitro multiplex assays with PBMCs
7. **Supplementary Table S6.** Demographics and clinical variables of MS patients and controls
8. **Supplementary Table S7.** List of co-druggable interactions and co-druggability score
9. **Supplementary Table S8.** Predicted targets for combination therapy
10. **Supplementary Figure S1.** Phosphoproteomics normalization pipeline
11. **Supplementary Figure S2.** Signaling activity of each interaction

Legends supplementary figures

Figure S1. Phosphoproteomics normalization pipeline. The graph shows the normalization algorithm developed to identify and select the significantly phosphorylated measurements, and normalize them accordingly to allow Boolean modeling.

Figure S2. Signaling activity of each interaction. Bars represent the signaling activity of each interaction for each donor subgroup, after merging the models for each individual patient by the mean across subgroups. Each one of the 5 panel shows the signaling activity of each interaction upon one of the 5 drug treatment against the activity in Healthy donors (grey) and Untreated patients (Orange). The thresholds show the upper quartile of each group mean defining as signaling noise the interactions with signaling activity below that threshold.

References

Abram, Clare L., and Clifford A. Lowell. 2009. "The Ins and Outs of Leukocyte Integrin Signaling." *Annual Review of Immunology* 27: 339–62.

Arish, Mohd, Mohammed Alaidarous, Rahat Ali, Yusuf Akhter, and Abdur Rub. 2017. "Implication of Sphingosine-1-Phosphate Signaling in Diseases: Molecular Mechanism and Therapeutic Strategies." *Journal of Receptor and Signal Transduction Research* 37 (5): 437–46.

Bayat Mokhtari, Reza, Tina S. Homayouni, Narges Baluch, Evgeniya Morgatskaya, Sushil Kumar, Bikul Das, and Herman Yeger. 2017. "Combination Therapy in Combating Cancer." *Oncotarget* 8 (23): 38022–43.

Bendall, Sean C., Garry P. Nolan, Mario Roederer, and Pratip K. Chattopadhyay. 2012. "A Deep Profiler's Guide to Cytometry." *Trends in Immunology* 33 (7): 323–32.

Bernardo-Faura, Marti, Stefan Massen, Christine S. Falk, Nathan R. Brady, and Roland Eils. 2014. "Data-Derived Modeling Characterizes Plasticity of MAPK Signaling in Melanoma." *PLoS Computational Biology* 10 (9): e1003795.

Beyer, Tilo, Mandy Busse, Kroum Hristov, Slavyana Gurbiel, Michal Smida, Utz-Uwe Haus, Kathrin Ballerstein, et al. 2011. "Integrating Signals from the T-Cell Receptor and the Interleukin-2 Receptor." *PLoS Computational Biology* 7 (8): e1002121.

Bozic, Ivana, Johannes G. Reiter, Benjamin Allen, Tibor Antal, Krishnendu Chatterjee, Preya Shah, Yo Sup Moon, et al. 2013. "Evolutionary Dynamics of Cancer in Response to Targeted Combination Therapy." *eLife* 2 (June): e00747.

Bulusu, Krishna C., Rajarshi Guha, Daniel J. Mason, Richard P. I. Lewis, Eugene Muratov, Yasaman Kalantar Motamedi, Murat Cokol, and Andreas Bender. 2016. "Modelling of Compound Combination Effects and Applications to Efficacy and Toxicity:

State-of-the-Art, Challenges and Perspectives." *Drug Discovery Today* 21 (2): 225–38.

Canto, Ester, Noriko Isobe, Alessandro Didonna, MS-EPIC Study Group, Stephen L. Hauser, and Jorge R. Oksenberg. 2018. "Aberrant STAT Phosphorylation Signaling in Peripheral Blood Mononuclear Cells from Multiple Sclerosis Patients." *Journal of Neuroinflammation* 15 (1): 72.

Chen, Ding, Sara J. Ireland, Gina Remington, Enrique Alvarez, Michael K. Racke, Benjamin Greenberg, Elliot M. Frohman, and Nancy L. Monson. 2016. "CD40-Mediated NF-κB Activation in B Cells Is Increased in Multiple Sclerosis and Modulated by Therapeutics." *Journal of Immunology* 197 (11): 4257–65.

Cokelaer, Thomas, Dennis Pultz, Lea M. Harder, Jordi Serra-Musach, and Julio Saez-Rodriguez. 2013. "BioServices: A Common Python Package to Access Biological Web Services Programmatically." *Bioinformatics* 29 (24): 3241–42.

Conway, Devon, and Jeffrey A. Cohen. 2010. "Combination Therapy in Multiple Sclerosis." *Lancet Neurology* 9 (3): 299–308.

Crespo, Isaac, Lou Götz, Robin Liechti, George Coukos, Marie-Agnès Doucey, and Ioannis Xenarios. 2016. "Identifying Biological Mechanisms for Favorable Cancer Prognosis Using Non-Hypothesis-Driven Iterative Survival Analysis." *NPJ Systems Biology and Applications* 2 (December): 16037.

Cully, Megan. 2015. "Combinations with Checkpoint Inhibitors at Wavefront of Cancer Immunotherapy." *Nature Reviews. Drug Discovery* 14 (6): 374–75.

Davis, Mark M., Cristina M. Tato, and David Furman. 2017. "Systems Immunology: Just Getting Started." *Nature Immunology* 18 (7): 725–32.

Eduati, Federica, Victoria Doldàn-Martelli, Bertram Klinger, Thomas Cokelaer, Anja Sieber, Fiona Kogera, Mathurin Dorel, Mathew J. Garnett, Nils Blüthgen, and Julio Saez-Rodriguez. 2017. "Drug Resistance Mechanisms in Colorectal Cancer Dissected with Cell Type-Specific Dynamic Logic Models." *Cancer Research* 77 (12): 3364–75.

Flobak, Åsmund, Anaïs Baudot, Elisabeth Remy, Liv Thommesen, Denis Thieffry, Martin Kuiper, and Astrid Lægreid. 2015. "Discovery of Drug Synergies in Gastric Cancer Cells Predicted by Logical Modeling." *PLoS Computational Biology* 11 (8): e1004426.

Galisteo, M. L., I. Dikic, A. G. Batzer, W. Y. Langdon, and J. Schlessinger. 1995. "Tyrosine Phosphorylation of the c-Cbl Proto-Oncogene Protein Product and Association with Epidermal Growth Factor (EGF) Receptor upon EGF Stimulation." *The Journal of Biological Chemistry* 270 (35): 20242–45.

Halasz, Melinda, Boris N. Kholodenko, Walter Kolch, and Tapesh Santra. 2016. "Integrating Network Reconstruction with Mechanistic Modeling to Predict Cancer Therapies." *Science Signaling* 9 (455): ra114.

Hassan, Namir J., Stephen J. Simmonds, Nicholas G. Clarkson, Sarah Hanrahan, Michael J. Puklavec, Martine Bomb, A. Neil Barclay, and Marion H. Brown. 2006. "CD6 Regulates T-Cell Responses through Activation-Dependent Recruitment of the Positive Regulator SLP-76." *Molecular and Cellular Biology* 26 (17): 6727–38.

Housley, William J., Salvador D. Fernandez, Kenneth Vera, Sasidhar R. Murikinati, Jaime Grutzendler, Nicole Cuerdon, Laura Glick, et al. 2015. "Genetic Variants Associated with Autoimmunity Drive NFκB Signaling and Responses to Inflammatory Stimuli." *Science Translational Medicine* 7 (291): 291ra93.

Hussman, J. P., A. H. Beecham, M. Schmidt, E. R. Martin, J. L. McCauley, J. M. Vance, J. L. Haines, and M. A. Pericak-Vance. 2016. "GWAS Analysis Implicates NF-κB-Mediated Induction of Inflammatory T Cells in Multiple Sclerosis." *Genes and Immunity* 17 (5): 305–12.

International Multiple Sclerosis Genetics Consortium (IMSGC), Ashley H. Beecham, Nikolaos

A. Patsopoulos, Dionysia K. Xifara, Mary F. Davis, Anu Kemppinen, Chris Cotsapas, et al. 2013. "Analysis of Immune-Related Loci Identifies 48 New Susceptibility Variants for Multiple Sclerosis." *Nature Genetics* 45 (11): 1353–60.

International Multiple Sclerosis Genetics Consortium, Wellcome Trust Case Control Consortium 2, Stephen Sawcer, Garrett Hellenthal, Matti Pirinen, Chris C. A. Spencer, Nikolaos A. Patsopoulos, et al. 2011. "Genetic Risk and a Primary Role for Cell-Mediated Immune Mechanisms in Multiple Sclerosis." *Nature* 476 (7359): 214–19.

Jia, Jia, Feng Zhu, Xiaohua Ma, Zhiwei Cao, Zhiwei W. Cao, Yixue Li, Yixue X. Li, and Yu Zong Chen. 2009. "Mechanisms of Drug Combinations: Interaction and Network Perspectives." *Nature Reviews. Drug Discovery* 8 (2): 111–28.

Johnson, B. A., J. Wang, E. M. Taylor, S. J. Caillier, J. Herbert, O. A. Khan, A. H. Cross, et al. 2010. "Multiple Sclerosis Susceptibility Alleles in African Americans." *Genes and Immunity* 11 (4): 343–50.

Kholodenko, Boris N. 2006. "Cell-Signalling Dynamics in Time and Space." *Nature Reviews. Molecular Cell Biology* 7 (3): 165–76.

Kholodenko, Boris N., John F. Hancock, and Walter Kolch. 2010. "Signalling Ballet in Space and Time." *Nature Reviews. Molecular Cell Biology* 11 (6): 414–26.

Kieseier, Bernd C., and Olaf Stüve. 2011. "Multiple Sclerosis: Combination Therapy in MS--Still a Valid Strategy." *Nature Reviews. Neurology* 7 (12): 659–60.

Klinger, Bertram, Anja Sieber, Raphaela Fritsche-Guenther, Franziska Witzel, Leanne Berry, Dirk Schumacher, Yibing Yan, et al. 2013. "Network Quantification of EGFR Signaling Unveils Potential for Targeted Combination Therapy." *Molecular Systems Biology* 9: 673.

Kolch, Walter, Melinda Halasz, Marina Granovskaya, and Boris N. Kholodenko. 2015. "The Dynamic Control of Signal Transduction Networks in Cancer Cells." *Nature Reviews. Cancer* 15 (9): 515–27.

Korkut, Anil, Weiqing Wang, Emek Demir, Bülent Arman Aksoy, Xiaohong Jing, Evan J. Molinelli, Özgün Babur, et al. 2015. "Perturbation Biology Nominates Upstream-Downstream Drug Combinations in RAF Inhibitor Resistant Melanoma Cells." *eLife* 4 (August). https://doi.org/10.7554/eLife.04640.

Kotelnikova, Ekaterina, Marti Bernardo-Faura, Gilad Silberberg, Narsis A. Kiani, Dimitris Messinis, Ioannis N. Melas, Laura Artigas, et al. 2015. "Signaling Networks in MS: A Systems-Based Approach to Developing New Pharmacological Therapies." *Multiple Sclerosis* 21 (2): 138–46.

Lee, Michael J., Albert S. Ye, Alexandra K. Gardino, Anne Margriet Heijink, Peter K. Sorger, Gavin MacBeath, and Michael B. Yaffe. 2012. "Sequential Application of Anticancer Drugs Enhances Cell Death by Rewiring Apoptotic Signaling Networks." *Cell* 149 (4): 780–94.

Lublin, Fred D., Stephen C. Reingold, Jeffrey A. Cohen, Gary R. Cutter, Per Soelberg Sørensen, Alan J. Thompson, Jerry S. Wolinsky, et al. 2014. "Defining the Clinical Course of Multiple Sclerosis: The 2013 Revisions." *Neurology* 83 (3): 278–86.

Luo, Bing-Hao, Christopher V. Carman, and Timothy A. Springer. 2007. "Structural Basis of Integrin Regulation and Signaling." *Annual Review of Immunology* 25: 619–47.

Martinez-Forero, Ivan, Ricardo Garcia-Munoz, Sara Martinez-Pasamar, Susana Inoges, Ascensión Lopez-Diaz de Cerio, Ricardo Palacios, Jorge Sepulcre, et al. 2008. "IL-10 Suppressor Activity and Ex Vivo Tr1 Cell Function Are Impaired in Multiple Sclerosis." *European Journal of Immunology* 38 (2): 576–86.

Martinez-Pasamar, Sara, Elena Abad, Beatriz Moreno, Nieves Velez de Mendizabal, Ivan Martinez-Forero, Jordi Garcia-Ojalvo, and Pablo Villoslada. 2013. "Dynamic Cross-Regulation of Antigen-Specific Effector and Regulatory T Cell Subpopulations and

Microglia in Brain Autoimmunity." *BMC Systems Biology* 7 (April): 34.

Meldal, Birgit H. M., Oscar Forner-Martinez, Maria C. Costanzo, Jose Dana, Janos Demeter, Marine Dumousseau, Selina S. Dwight, et al. 2015. "The Complex Portal--an Encyclopaedia of Macromolecular Complexes." *Nucleic Acids Research* 43 (Database issue): D479–84.

Milo, Ron, and Hillel Panitch. 2011. "Combination Therapy in Multiple Sclerosis." *Journal of Neuroimmunology* 231 (1-2): 23–31.

Moreno, Beatriz, Henar Hevia, Monica Santamaria, Jorge Sepulcre, Javier Muñoz, Elena R. García-Trevijano, Carmen Berasain, Fernando J. Corrales, Matias A. Avila, and Pablo Villoslada. 2006. "Methylthioadenosine Reverses Brain Autoimmune Disease." *Annals of Neurology* 60 (3): 323–34.

Morris, Melody K., An Chi, Ioannis N. Melas, and Leonidas G. Alexopoulos. 2014. "Phosphoproteomics in Drug Discovery." *Drug Discovery Today* 19 (4): 425–32.

Owens, Joanna. 2007. "Determining Druggability." *Nature Reviews. Drug Discovery* 6 (3): 187–187.

Palacios, Ricardo, Joaquin Goni, Ivan Martinez-Forero, Jaime Iranzo, Jorge Sepulcre, Ignacio Melero, and Pablo Villoslada. 2007. "A Network Analysis of the Human T-Cell Activation Gene Network Identifies JAGGED1 as a Therapeutic Target for Autoimmune Diseases." *PloS One* 2 (11): e1222.

Pertsovskaya, Inna, Elena Abad, Núria Domedel-Puig, Jordi Garcia-Ojalvo, and Pablo Villoslada. 2013. "Transient Oscillatory Dynamics of Interferon Beta Signaling in Macrophages." *BMC Systems Biology* 7 (July): 59.

Polman, Chris H., Stephen C. Reingold, Gilles Edan, Massimo Filippi, Hans-Peter Hartung, Ludwig Kappos, Fred D. Lublin, et al. 2005. "Diagnostic Criteria for Multiple Sclerosis: 2005 Revisions to the 'McDonald Criteria.'" *Annals of Neurology* 58 (6): 840–46.

Poussin, Carine, Carole Mathis, Leonidas G. Alexopoulos, Dimitris E. Messinis, Rémi H. J. Dulize, Vincenzo Belcastro, Ioannis N. Melas, et al. 2014. "The Species Translation Challenge-a Systems Biology Perspective on Human and Rat Bronchial Epithelial Cells." *Scientific Data* 1 (June): 140009.

Ransohoff, Richard M., David A. Hafler, and Claudia F. Lucchinetti. 2015. "Multiple Sclerosis-a Quiet Revolution." *Nature Reviews. Neurology* 11 (3): 134–42.

Rose, David M., Ronen Alon, and Mark H. Ginsberg. 2007. "Integrin Modulation and Signaling in Leukocyte Adhesion and Migration." *Immunological Reviews* 218 (August): 126–34.

Saez-Rodriguez, Julio, Leonidas G. Alexopoulos, Jonathan Epperlein, Regina Samaga, Douglas A. Lauffenburger, Steffen Klamt, and Peter K. Sorger. 2009. "Discrete Logic Modelling as a Means to Link Protein Signalling Networks with Functional Analysis of Mammalian Signal Transduction." *Molecular Systems Biology* 5 (December): 331.

Sanna, Serena, Maristella Pitzalis, Magdalena Zoledziewska, Ilenia Zara, Carlo Sidore, Raffaele Murru, Michael B. Whalen, et al. 2010. "Variants within the Immunoregulatory CBLB Gene Are Associated with Multiple Sclerosis." *Nature Genetics* 42 (6): 495–97.

Schneider, William M., Meike Dittmann Chevillotte, and Charles M. Rice. 2014. "Interferon-Stimulated Genes: A Complex Web of Host Defenses." *Annual Review of Immunology* 32 (February): 513–45.

Sellebjerg, F., M. Krakauer, M. Khademi, T. Olsson, and P. S. Sørensen. 2012. "FOXP3, CBLB and ITCH Gene Expression and Cytotoxic T Lymphocyte Antigen 4 Expression on CD4(+) CD25(high) T Cells in Multiple Sclerosis." *Clinical and Experimental Immunology* 170 (2): 149–55.

Silverbush, Dana, Shaun Grosskurth, Dennis Wang, Francoise Powell, Berthold Gottgens, Jonathan Dry, and Jasmin Fisher. 2017. "Cell-Specific Computational Modeling of the PIM

Pathway in Acute Myeloid Leukemia." *Cancer Research* 77 (4): 827–38.

Slavin-Chiorini, Dale C., Marta Catalfamo, Chie Kudo-Saito, James W. Hodge, Jeffrey Schlom, and Helen Sabzevari. 2004. "Amplification of the Lytic Potential of Effector/memory CD8+ Cells by Vector-Based Enhancement of ICAM-1 (CD54) in Target Cells: Implications for Intratumoral Vaccine Therapy." *Cancer Gene Therapy* 11 (10): 665–80.

Stürner, Klarissa Hanja, Uwe Borgmeyer, Christian Schulze, Ole Pless, and Roland Martin. 2014. "A Multiple Sclerosis–Associated Variant of CBLB Links Genetic Risk with Type I IFN Function." *The Journal of Immunology* 193 (9): 4439–47.

Swaminathan, Gayathri, and Alexander Y. Tsygankov. 2006. "The Cbl Family Proteins: Ring Leaders in Regulation of Cell Signaling." *Journal of Cellular Physiology* 209 (1): 21–43.

Takuwa, Yoh, Yasuo Okamoto, Kazuaki Yoshioka, and Noriko Takuwa. 2012. "Sphingosine-1-Phosphate Signaling in Physiology and Diseases." *BioFactors* 38 (5): 329–37.

Tarcic, Gabi, Shlomit K. Boguslavsky, Jean Wakim, Tai Kiuchi, Angela Liu, Felicia Reinitz, David Nathanson, et al. 2009. "An Unbiased Screen Identifies DEP-1 Tumor Suppressor as a Phosphatase Controlling EGFR Endocytosis." *Current Biology: CB* 19 (21): 1788–98.

Terfve, Camille, Thomas Cokelaer, David Henriques, Aidan MacNamara, Emanuel Goncalves, Melody K. Morris, Martijn van Iersel, Douglas A. Lauffenburger, and Julio Saez-Rodriguez. 2012. "CellNOptR: A Flexible Toolkit to Train Protein Signaling Networks to Data Using Multiple Logic Formalisms." *BMC Systems Biology* 6 (October): 133.

Vaga, S., M. Bernardo-Faura, T. Cokelaer, A. Maiolica, C. A. Barnes, L. C. Gillet, B. Hegemann, et al. 2014. "Phosphoproteomic Analyses Reveal Novel Cross-Modulation Mechanisms between Two Signaling Pathways in Yeast." *Molecular Systems Biology* 10 (12): 767–767.

Villoslada, Pablo, Lawrence Steinman, and Sergio E. Baranzini. 2009. "Systems Biology and Its Application to the Understanding of Neurological Diseases." *Annals of Neurology* 65 (2): 124–39.

A Identify subgroup networks

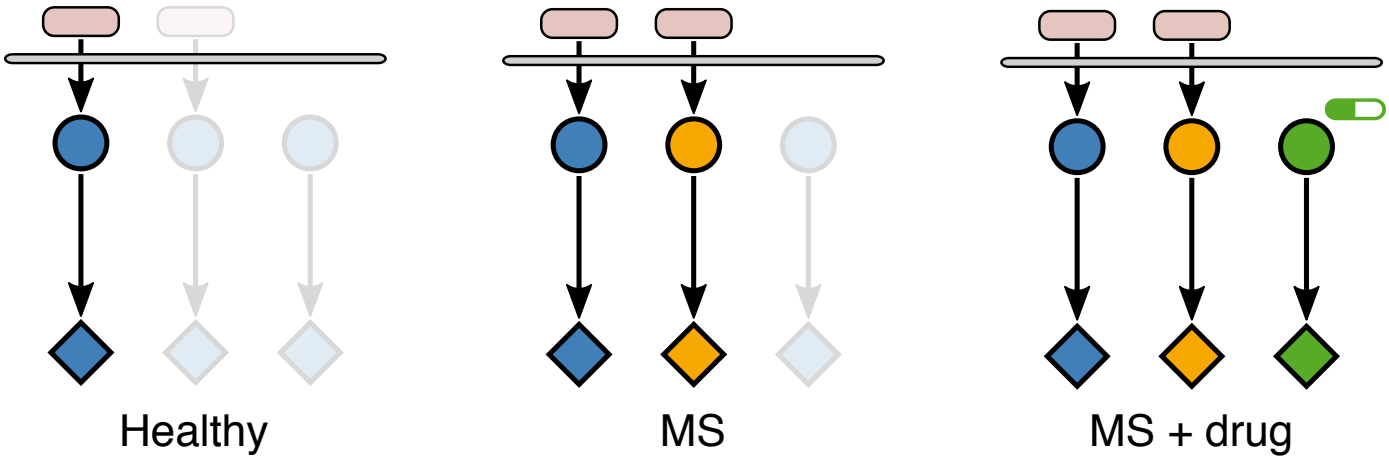

B Score all subgroup reactions to find co-druggable

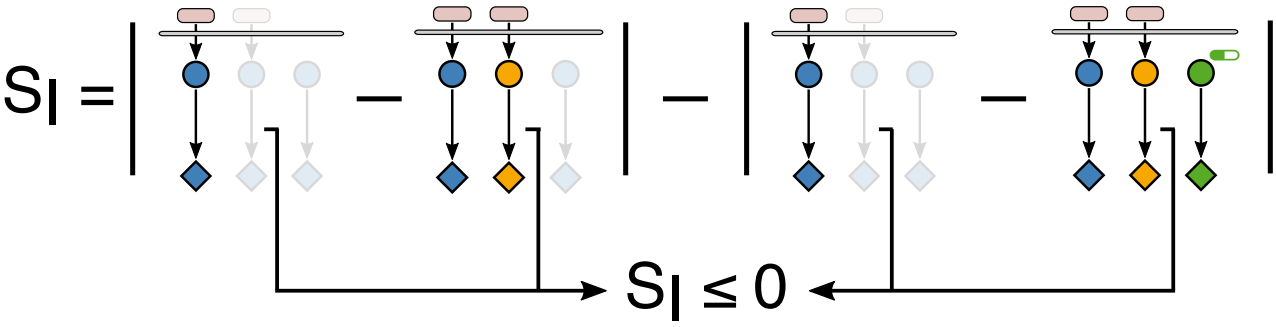

C Topological prediction of drug combination

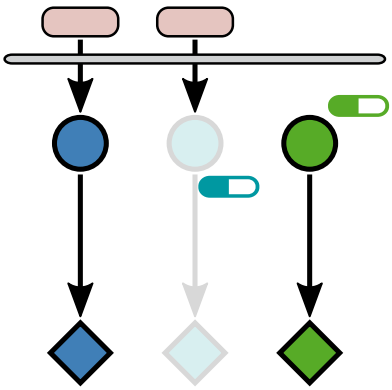

Figure 1

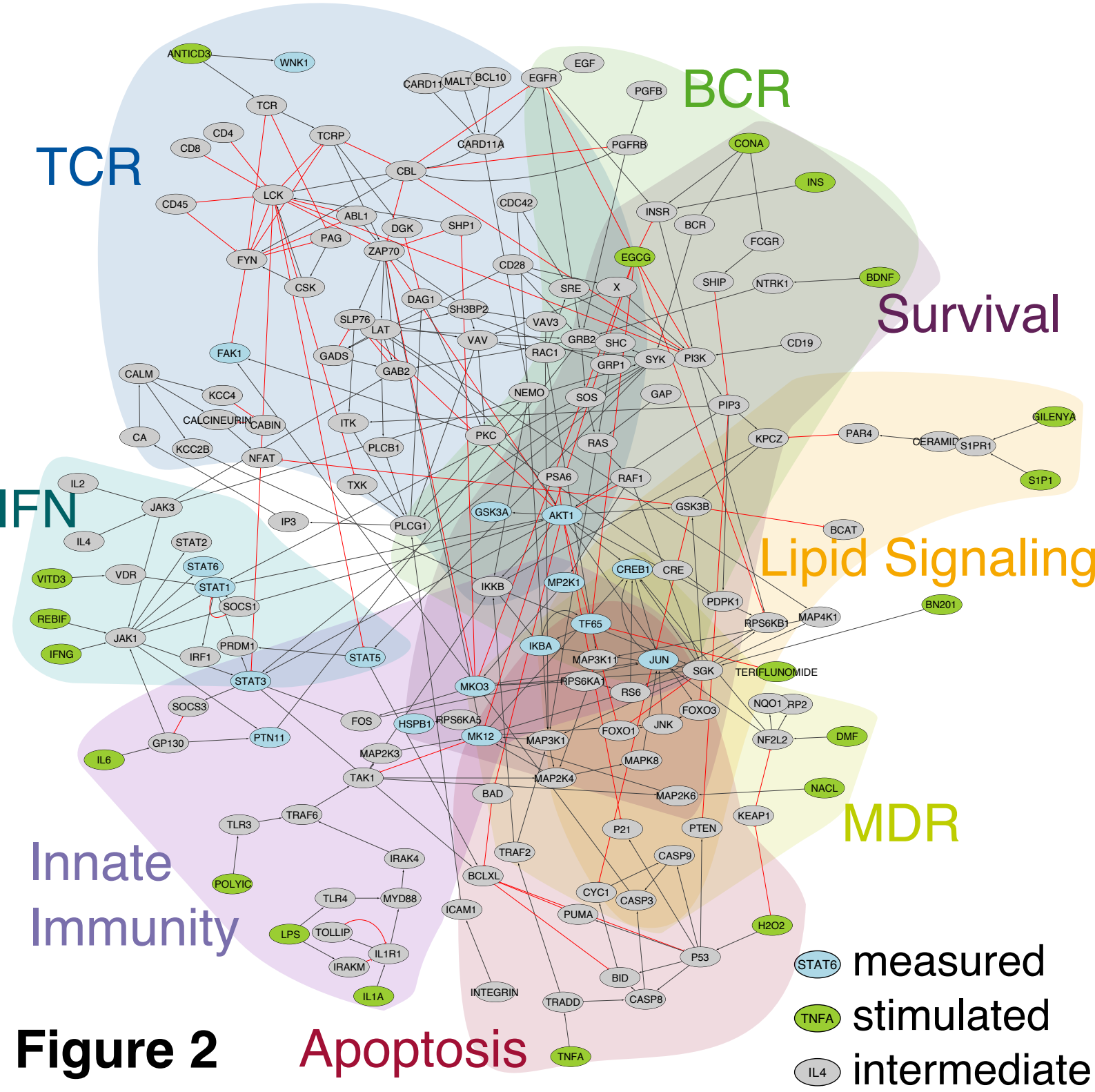
TCR
BCR
Survival
IFN
Lipid Signaling
MDR
Innate Immunity
Apoptosis
ANTICD3
WNK1
TCR
CD4
CD8
TCRP
CD45
LCK
CBL
CARD11
MALT
BCL10
EGFR
EGF
PGFB
PGFRB
CARD11A
CONA
INS
INSR
BCR
FCGR
ABL1
DGK
SHP1
PAG
ZAP70
FYN
CSK
CDC42
CD28
EGCG
SHIP
NTRK1
BDNF
SRE
X
DAG1
SH3BP2
SLP76
LAT
VAV3
VAV
GRB2
SHC
RAC1
GRP1
SYK
PI3K
CD19
FAK1
GADS
GAB2
CALM
KCC4
CALCINEURIN
CABIN
CA
KCC2B
NFAT
ITK
PLCB1
NEMO
SOS
GAP
PIP3
PKC
RAS
KPCZ
PAR4
CERAMID
S1PR1
GILENYA
S1P1
PSA6
RAF1
TXK
IL2
JAK3
IL4
IP3
PLCG1
GSK3A
AKT1
GSK3B
BCAT
STAT2
STAT6
VITD3
VDR
STAT1
SOCS1
REBIF
JAK1
IFNG
IRF1
PRDM1
STAT5
STAT3
CREB1
CRE
IKKB
MP2K1
PDPK1
RPS6KB1
MAP4K1
BN201
TF65
IKBA
MAP3K11
JUN
SGK
TERIFLUNOMIDE
MKO3
RPS6KA1
RS6
SOCS3
FOS
HSPB1
RPS6KA5
FOXO3
NQO1
RP2
GP130
PTN11
MK12
MAP3K1
FOXO1
JNK
NF2L2
DMF
IL6
MAP2K3
MAPK8
TAK1
MAP2K4
BAD
MAP2K6
NACL
TRAF6
TLR3
KEAP1
P21
PTEN
IRAK4
TRAF2
CASP9
POLYIC
BCLXL
CYC1
CASP3
TLR4
MYD88
ICAM1
PUMA
H2O2
LPS
TOLLIP
IL1R1
IRAKM
P53
BID
IL1A
INTEGRIN
TRADD
CASP8
TNFA
STAT6 measured
TNFA stimulated
IL4 intermediate

Figure 2

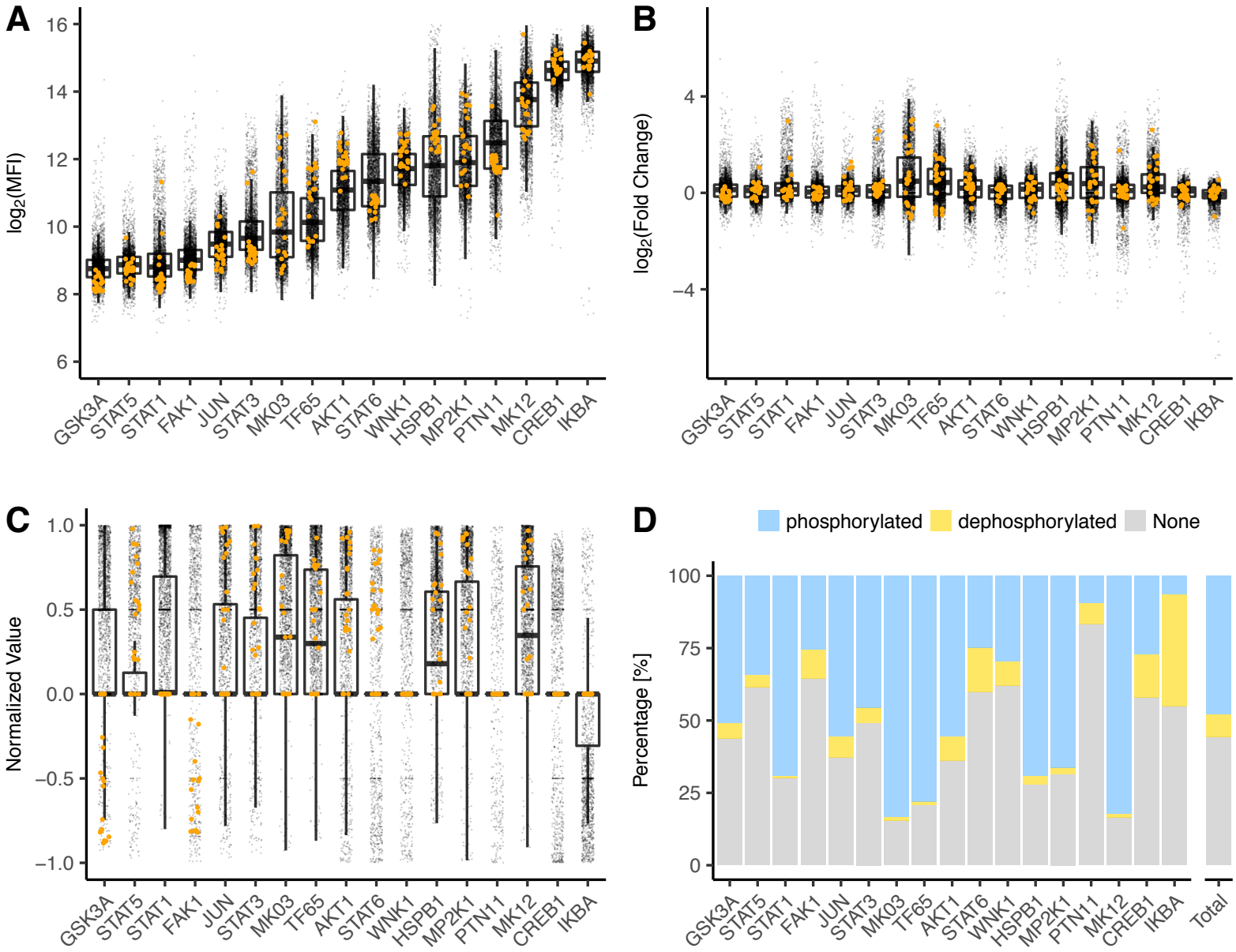
A
log2(MFI)
16
14
12
10
8
6
GSK3A
STAT5
STAT1
FAK1
JUN
STAT3
MK03
TF65
AKT1
STAT6
WNK1
HSPB1
MP2K1
PTN11
MK12
CREB1
IKBA
B
log2(Fold Change)
4
0
−4
C
Normalized Value
1.0
0.5
0.0
−0.5
−1.0
D
phosphorylated
dephosphorylated
None
Percentage [%]
100
75
50
25
0
Total

Figure 3

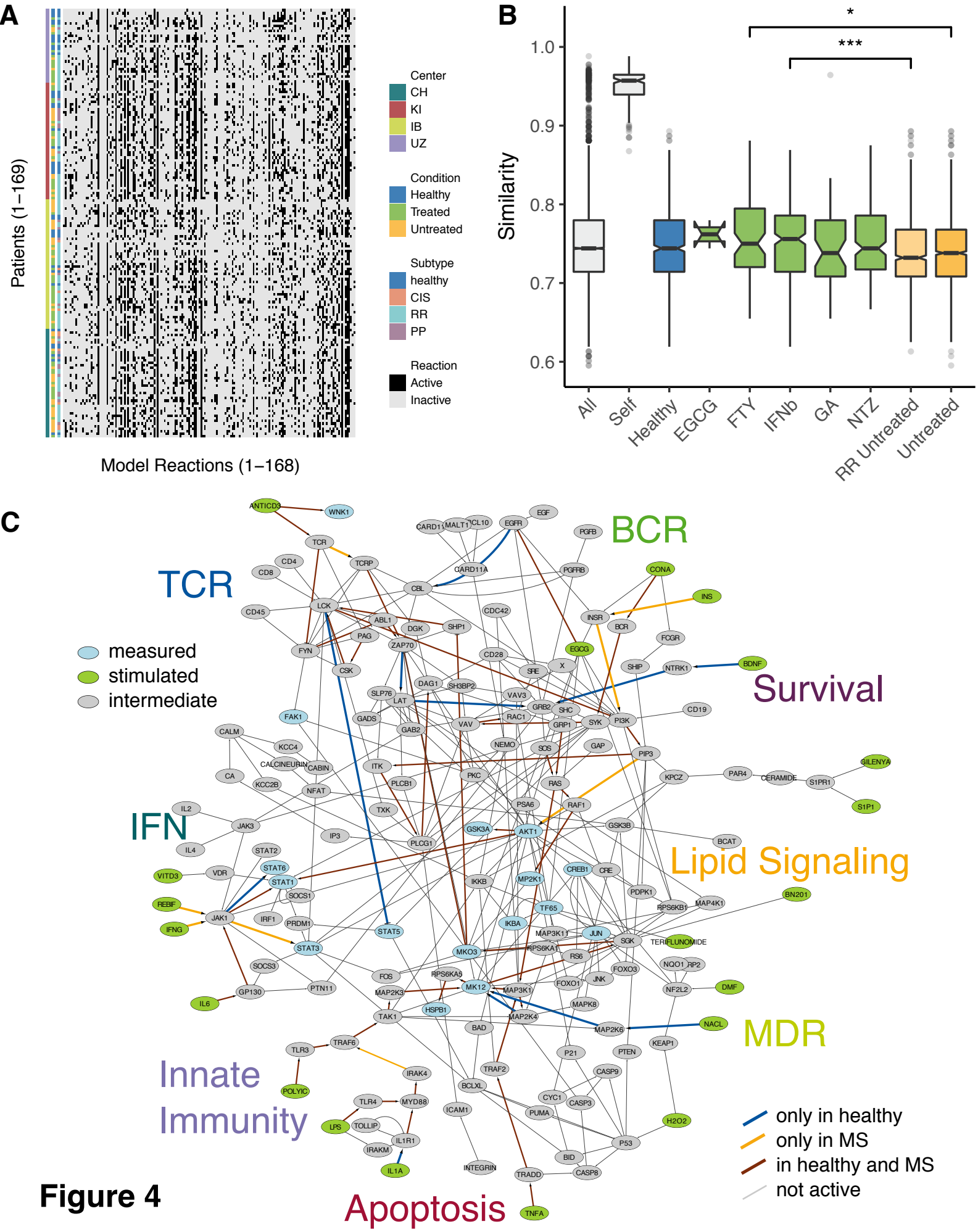
A
Patients (1–169)
Model Reactions (1–168)
Center
CH
KI
IB
UZ
Condition
Healthy
Treated
Untreated
Subtype
healthy
CIS
RR
PP
Reaction
Active
Inactive
B
Similarity
1.0
0.9
0.8
0.7
0.6
*
***
All
Self
Healthy
EGCG
FTY
IFNb
GA
NTZ
RR Untreated
Untreated
C
measured
stimulated
intermediate
TCR
BCR
Survival
IFN
Lipid Signaling
MDR
Innate Immunity
Apoptosis
only in healthy
only in MS
in healthy and MS
not active

Figure 4

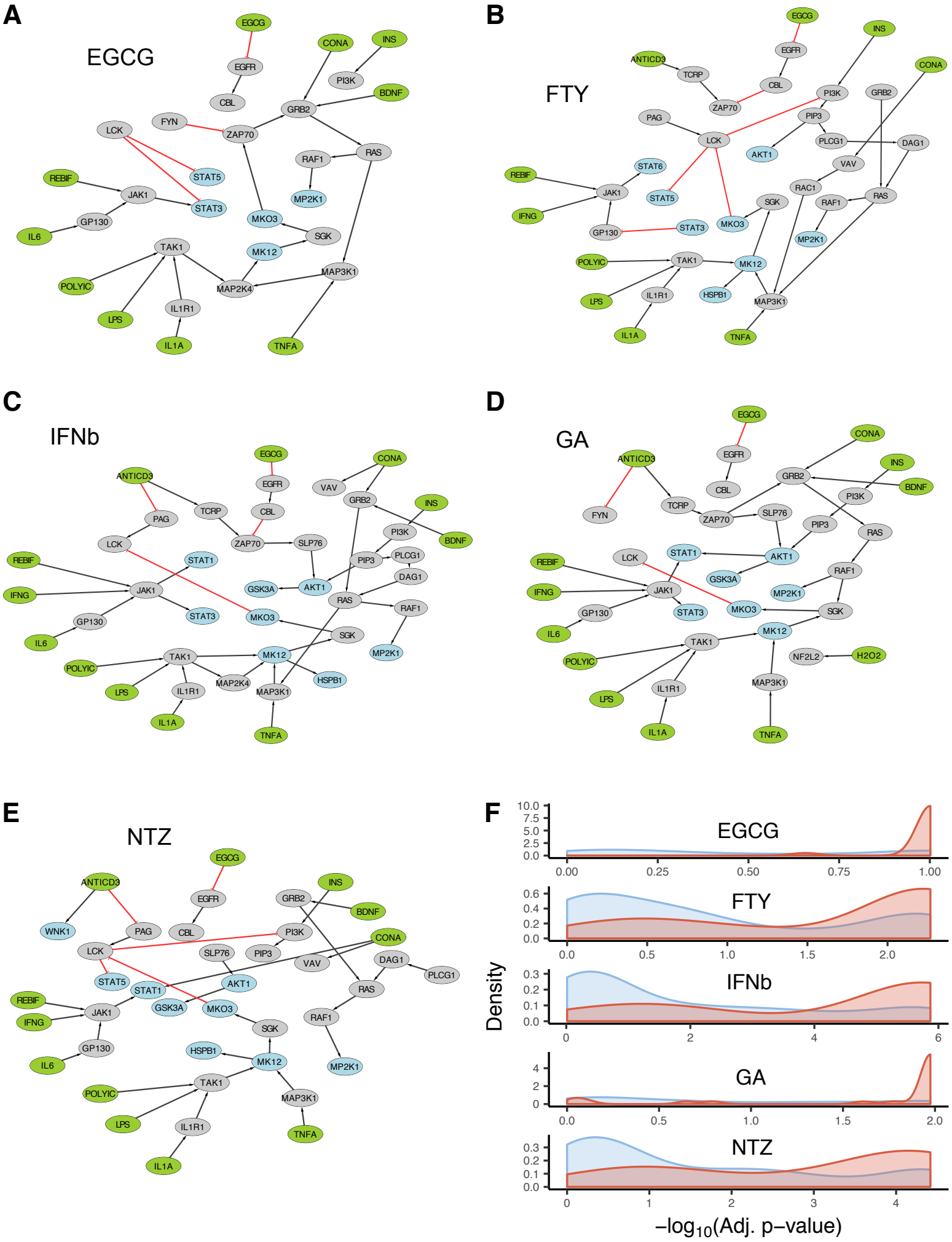
A
EGCG
EGCG
EGFR
CBL
CONA
INS
PI3K
BDNF
GRB2
FYN
ZAP70
LCK
RAS
RAF1
STAT5
REBIF
JAK1
STAT3
MP2K1
GP130
MKO3
IL6
SGK
TAK1
MK12
MAP3K1
POLYIC
MAP2K4
IL1R1
LPS
IL1A
TNFA
B
FTY
EGCG
INS
EGFR
ANTICD3
TCRP
CONA
CBL
PI3K
GRB2
ZAP70
PAG
PIP3
LCK
PLCG1
DAG1
AKT1
VAV
STAT6
REBIF
RAC1
JAK1
STAT5
RAS
SGK
RAF1
IFNG
MKO3
GP130
STAT3
MP2K1
POLYIC
TAK1
MK12
LPS
IL1R1
HSPB1
MAP3K1
IL1A
TNFA
C
IFNb
EGCG
CONA
ANTICD3
EGFR
VAV
GRB2
INS
TCRP
CBL
PAG
PI3K
BDNF
LCK
ZAP70
SLP76
REBIF
STAT1
PIP3
PLCG1
DAG1
IFNG
JAK1
GSK3A
AKT1
RAS
GP130
STAT3
MKO3
RAF1
IL6
SGK
MP2K1
TAK1
MK12
POLYIC
HSPB1
MAP2K4
LPS
IL1R1
MAP3K1
IL1A
TNFA
D
GA
EGCG
CONA
ANTICD3
EGFR
INS
GRB2
BDNF
CBL
PI3K
TCRP
FYN
ZAP70
SLP76
PIP3
RAS
LCK
STAT1
AKT1
REBIF
GSK3A
RAF1
IFNG
JAK1
MP2K1
GP130
STAT3
MKO3
SGK
IL6
MK12
TAK1
NF2L2
H2O2
POLYIC
MAP3K1
IL1R1
LPS
IL1A
TNFA
E
NTZ
EGCG
ANTICD3
INS
EGFR
GRB2
BDNF
WNK1
PAG
CBL
PI3K
CONA
LCK
SLP76
PIP3
VAV
DAG1
PLCG1
STAT5
STAT1
AKT1
RAS
REBIF
GSK3A
MKO3
JAK1
IFNG
RAF1
SGK
GP130
HSPB1
MK12
MP2K1
IL6
TAK1
POLYIC
MAP3K1
LPS
IL1R1
TNFA
IL1A
F
EGCG
FTY
IFNb
GA
NTZ
Density
–log10(Adj. p–value)

Figure 5

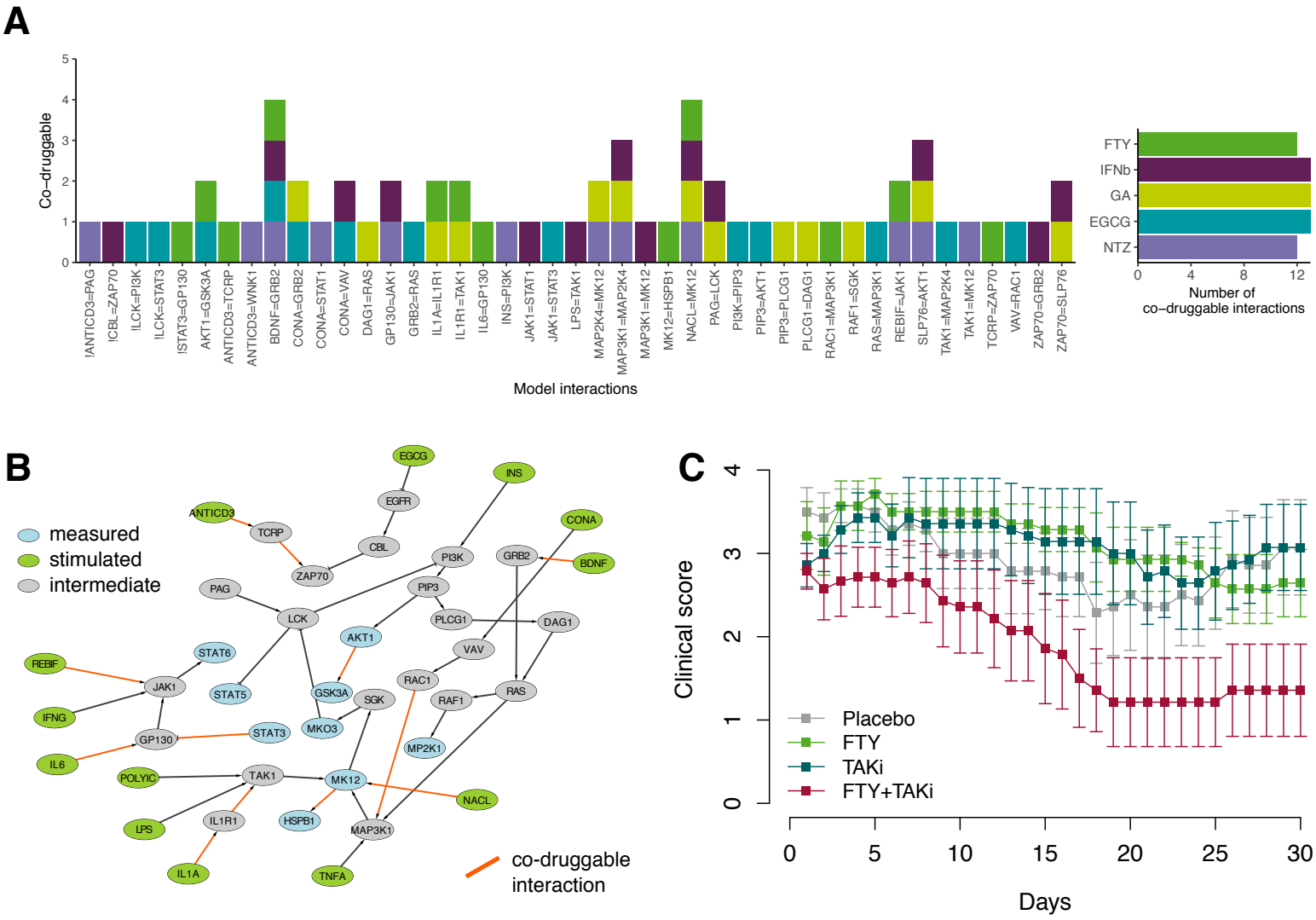
A
Co−druggable
Model interactions
!ANTICD3=PAG
!CBL=ZAP70
!LCK=PI3K
!LCK=STAT3
!STAT3=GP130
AKT1=GSK3A
ANTICD3=TCRP
ANTICD3=WNK1
BDNF=GRB2
CONA=GRB2
CONA=STAT1
CONA=VAV
DAG1=RAS
GP130=JAK1
GRB2=RAS
IL1A=IL1R1
IL1R1=TAK1
IL6=GP130
INS=PI3K
JAK1=STAT1
JAK1=STAT3
LPS=TAK1
MAP2K4=MK12
MAP3K1=MAP2K4
MAP3K1=MK12
MK12=HSPB1
NACL=MK12
PAG=LCK
PI3K=PIP3
PIP3=AKT1
PIP3=PLCG1
PLCG1=DAG1
RAC1=MAP3K1
RAF1=SGK
RAS=MAP3K1
REBIF=JAK1
SLP76=AKT1
TAK1=MAP2K4
TAK1=MK12
TCRP=ZAP70
VAV=RAC1
ZAP70=GRB2
ZAP70=SLP76
FTY
IFNb
GA
EGCG
NTZ
Number of co−druggable interactions
B
measured
stimulated
intermediate
co-druggable interaction
EGCG
INS
EGFR
ANTICD3
TCRP
CONA
CBL
PI3K
GRB2
BDNF
ZAP70
PAG
PIP3
LCK
PLCG1
DAG1
AKT1
VAV
STAT6
REBIF
JAK1
STAT5
GSK3A
SGK
RAC1
RAS
RAF1
IFNG
MKO3
STAT3
GP130
MP2K1
IL6
POLYIC
TAK1
MK12
NACL
LPS
IL1R1
HSPB1
MAP3K1
IL1A
TNFA
C
Clinical score
Days
Placebo
FTY
TAKi
FTY+TAKi

Figure 6

Healthy	MS	Treated	Score	Treatment affecting?	Healthy-like signaling after treatment?
0	0	0	0		
0	0	1	-1		
0	1	0	1		
0	1	1	0		
1	0	0	0		
1	0	1	1		
1	1	0	-1		
1	1	1	0		

Yes

No

Effective Treatment

Co-druggable (Treatment is affecting)

Co-druggable (Treatment is not affecting)

Table 1